

Available online at website: https://journal.bcrec.id/index.php/bcrec

Bulletin of Chemical Reaction Engineering & Catalysis, 19 (4) 2024, 560-572



Research Article

CuAl-LDH Modified with Filamentous Macroalgae for Anionic Dyes Removal: A Study on Selectivity, Adsorption Efficiency, and Regeneration

Alfan Wijaya^{1,2}, Laila Hanum³, Elda Melwita^{4,5}, Aldes Lesbani^{2,5*}

¹Doctoral Program of Environmental Sciences, Graduate School, Universitas Sriwijaya, Palembang, South Sumatera, 30139, Indonesia

²Research Centre of Inorganic Materials and Coordination Complexes, Universitas Sriwijaya, Palembang, South Sumatera, 30139, Indonesia

³Department of Biology, Faculty of Mathematics and Natural Sciences, Universitas Sriwijaya, Ogan Ilir, South Sumatera, 30862, Indonesia

⁴Department of Chemical Engineering, Faculty of Mathematics and Natural Sciences, Universitas Sriwijaya, Ogan Ilir, South Sumatera, 30862, Indonesia

⁵Master Program of Material Science, Graduate School, Universitas Sriwijaya, Palembang, South Sumatera, 30139, Indonesia

Received: 1th October 2024; Revised: 30th October 2024; Accepted: 30th October 2024 Available online: 10th November 2024; Published regularly: December 2024



Abstract

Continuous modifications of Layered Double Hydroxides (LDH) materials are essential to enhance their structural stability and improve their capacity for pollutant adsorption, addressing the need for more effective remediation strategies in environmental applications. This research study has proposed the preparation of CuAl-LDH supported filamentous macroalgae of Spirogyra sp. (CuAl-LDH/SA) via coprecipitation and hydrothermal methods. The prepared CuAl-LDH/SA composites were investigated for the adsorption of direct yellow 12 (DY) and remazol red (RR) dyes in batch mode experiments. The structure and morphology of the prepared CuAl-LDH/SA were identified by X-ray Diffraction (XRD), Fourier Transform Infra Red (FT-IR), (Brunauer-Emmett-Teller) BET surface area, Thermogravimetry / Differential Thermal Analyzer (TG/DTA), and Scanning Electron Microscope (SEM). For the adsorption process, the effects of initial pH, contact time, initial concentration, temperature, adsorption selectivity, and adsorbent regeneration, as well as kinetics, isotherms, and thermodynamics were studied. The adsorption selectivity test resulted in the RR dye being more selective compared to DY. The maximum capacities for RR adsorption were 72.464 mg/g (pH = 2, 150 min, 303 K). CuAl-LDH/SA can be regenerated for 4 cycles with a percent removal of 29.32%. The adsorption process followed the intraparticle diffusion kinetics model and Langmuir isotherm. Thermodynamic studies showed that the adsorption of RR using CuAl-LDH/SA was endothermic and spontaneous. The results of this study indicate that CuAl-LDH/SA composite material shows potential material in the removal of anionic dyes from aqueous solutions.

Copyright © 2024 by Authors, Published by BCREC Publishing Group. This is an open access article under the CC BY-SA License (https://creativecommons.org/licenses/by-sa/4.0).

Keywords: CuAl-LDH; Spirogyra sp. algae; anionic dyes; selectivity; regeneration

How to Cite: Wijaya, A., Hanum, L., Melwita, E., Lesbani, A. (2024). CuAl-LDH Modified with Filamentous Macroalgae for Anionic Dyes Removal: A Study on Selectivity, Adsorption Efficiency, and Regeneration. Bulletin of Chemical Reaction Engineering & Catalysis, 19 (4), 560-572 (doi: 10.9767/bcrec.20223)

Permalink/DOI: https://doi.org/10.9767/bcrec.20223

1. Introduction

Concerns over environmental pollution are increasing along with industrial development. Water pollution is a significant threat to human

health, as it is one of the main contributors to environmental degradation. Water pollution affects various aspects of our ecosystem, including soil, air, and water quality. Water pollution has become a significant global issue in recent times, causing serious damage to aquatic ecosystems and

Email: aldeslesbani@pps.unsri.ac.id (A. Lesbani)

^{*} Corresponding Author.

jeopardizing human health and progress. Research shows that water-soluble dye pollution is a major complex contaminant found in aquatic environments [1,2]. Effluent discharged from industries such as textiles, cosmetics, and dyeing can have detrimental effects. The treatment of dyeing effluent has become a pressing concern, given the potential harm it poses to human health. Dyes can be categorised into three types based on their charges: cationic dyes, anionic dyes, and amphoteric ionic dyes [3]. There available numerous techniques for the elimination of dyes, such as membrane separation [4], coagulation-flocculation [5,6], photocatalytic [7,8], adsorption [9,10], etc. Adsorption is considered a highly effective technique for remediation of water pollutants. It offers easy operation, low cost, absence of toxic by-products, and recyclability, making it a promising option

Currently, there are many materials used in the adsorption process of dye wastewater treatment, such as rice husk, montmorillonite, hydrochar, humic acid, chitosan, lignin, magnetic material, and layered double hydroxide, etc. [3,13–16]. Layered double hydroxide (LDH) is a fascinating 2D layered material that shares similarities with hydrotalcite. In terms of structure, LDH closely resembles brucite. It is composed of metal cations arranged in octahedral layers, with hydroxides serving as ligands along the edges. LDH is composed of metal hydroxides with positive charges, which are arranged in layers with anions serving as charge balancers. These anions can include nitrate, carbonate, sulfate, chloride, and more [17,18]. Based on the literature, LDH has been widely used in dye removal processes due to its outstanding ion exchange and adsorption capabilities. However, LDH has the disadvantage of poor structural stability, which makes the reuse efficiency of the material unfavorable. Therefore, it is imperative to modify LDH materials by compositing them using support materials [10,19,20].

Previous research has successfully modified NiAl-LDH using supporting materials in the form of cellulose, resulting in a surface area of 5.096 m²/g and can be used repeatedly for 6 cycles with a percent removal of malachite green dye of 54% [9]. Modification of CuAl/LDH has been carried out with biochar from rice husk for malachite green dye removal and produced an adsorbent that can be reused three times with a percent removal of 72% [21]. Based on Han et al. [22] and Normah et al. [23] research, CuAl-LDH composited with carbon-based materials produces chemically stable LDH composites. Therefore, the development of LDH materials continues to be carried out to obtain materials that have high structural stability.

species, both Algae macroalgae microalgae, have garnered significant attention as a highly researched biomass worldwide. This is primarily due to their numerous advantages over terrestrial biomass. In recent years, macroalgae have been used as adsorbents to remove contaminants from aqueous solutions [24,25]. Macroalgae is a green and renewable resource. Spirogyra sp. is one kind of filamentous green macroalgae, which is widely found in surface water and waterlogged soil. Several studies have Spirogyra sp. can shown that contaminants in water [26]. Other studies have shown the success of *Spirogyra sp.* algae used as a support material for heavy metal ion removal applications [27]. Therefore, Spirogyra sp. algae is suitable for use as a supporting material in LDH material modification to improve the ability of composite materials. Several methods have been reported for the preparation of LDH composite materials with carbon-based materials. The most frequently used preparation method coprecipitation. Several types of LDHs and the resulting composites, or hybrids, have been prepared using this technique for various applications. Although this procedure is rather simple, it can be difficult to achieve wellstructured LDHs. So, an assistive method is needed for the successful synthesis of the material. Hydrothermal synthesis has been shown to improve material crystallization and can produce well-organized LDH sheets [28].

This study modified CuAl-LDH filamentous macroalgae of Spirogyra species via coprecipitation and hydrothermal for efficient adsorption of DY and RR dyes. The composites were characterized by XRD, FT-IR, BET surface area, TG/DTA, and SEM. Adsorption experiments were conducted with DY and RR dye solutions, in which the effects of pH, kinetics, isotherms, and thermodynamic parameters were evaluated. In addition, the adsorption selectivity and regeneration of the adsorbent also investigated.

2. Materials and Methods

2.1 Chemicals and Characterizations

Filamentous macroalgae of Spirogyra species collected from swamp waters in South Sumatra, Indonesia. Copper nitrate $(Cu(NO_3)_2 \cdot 3H_2O)$, aluminum nitrate $(Al(NO_3)_3 \cdot 9H_2O),$ sodium hydroxide (NaOH), and sodium chloride (NaCl) were purchased from Merck. Distilled water was obtained from PT. Brataco, Hydrochloric acid (HCl) was manufactured by MallinckrodtAR®. The dyes used in this study are direct yellow 12 (DY) and remazol red (RR).

Material characterization in this study includes X-ray diffractometer (Rigaku Miniflex-

6000), Fourier Transform Infra-Red Spectroscopy (Shimadzu Prestige-21), Brunaur-Emmett-Teller (BET) surface area method (Quantrachrome), and Thermal Thermogravimetry Differential Analysis. The XRD pattern was recorded from 3°-80°, The FT-IR spectra were throughout a wavenumber range from 4000-400 cm⁻¹, TG/DTA analysis was recorded from room temperature to 900 °C, the specific surface area and porosity of the samples were measured by N₂ adsorption-desorption isotherm, the surface area was calculated based on BET method, and morphological analysis of materials using Quanta 650 SEM-EDS apparatus. The material's pHpzc was determined using a 0.1 M NaCl solution, with initial pH values adjusted from 2 to 11. Samples for 12 hours, shaken followed by measurement of final pH, and a correlation graph between initial and final pH values was plotted.

2.2 Preparation of CuAl-LDH/SA Composite

The synthesis of CuAl-LDH followed the method reported by Normah et al. [23]. Modification of CuAl-LDH using coprecipitation and hydrothermal methods, where CuAl-LDH is in the gel phase and *Spirogyra* algae are in the solid/powder phase. The Spirogyra algae were washed with water and dried in an oven at 80 °C. Following that, the material was finely ground and then passed through a sieve with a mesh size of 100. A powder was created from Spirogyra algae. The preparation of CuAl-LDH/SA begins by mixing the two solutions containing 30 mL Cu(NO₃)₂·3H₂O 0.75 M and 30 mL Al(NO₃)₃·9H₂O 0.25 M in a beaker. The mixture was then adjusted to pH = 10 by gradually adding 2 M NaOH solution. Then, the mixture was stirred for 30 minutes at 80 °C for 15 minutes. Spirogyra algae powder was prepared and put 3 g into the mixture and stirred for 15 min. The mixture was put into a hydrothermal device and oven at 105 °C for 5 hours. Then, the mixture was vacuum filtered and dried in an oven at 80 °C, followed by grinding and sieved with a 100 mesh sieve. CuAl-LDH/SA composite materials have fabricated.

2.3 Adsorption, Selectivity, and Regeneration Studies

Adsorption studies were conducted examine the impact of various factors on the adsorption process using a batch adsorption system. These factors included pH, temperature, contact time, and initial concentration of the substances. Adsorption selectivity was performed by mixing the two dyes and performing the adsorption process with the aim of seeing which more selective. The adsorbent regeneration process in this study was carried out for 5 cycles to test the structural stability and

ability of the adsorbent to reuse in the adsorption process.

In each experiment, the concentration of dye solution used was 50 mg/L with 0.02 g adsorbent weight. The solution was mixed using a shaker at 120 rpm. Subsequently, the solution was analyzed using a UV-Vis spectrophotometer, specifically at a wavelength of 515 nm (RR) and 414 nm (DY). This study explored the pH range of 2-11 by adjusting the pH of the solution with 0.1 M HCl and 0.1 M NaOH solutions. A study of the effects of various initial concentrations and temperatures on the adsorption process was conducted with concentrations varying from 60-100 mg/L, while temperatures ranged from 303-323K.

The adsorbent regeneration study began with the adsorption process by first incorporating 0.02 g of adsorbent into 20 mL of dye solution. Afterward, the mixture was stirred using a shaker, followed by filtration to separate the solution from the adsorbent. The adsorbent was then desorbed by adding 20 mL of distilled water and assisted with ultrasonic equipment. The adsorbent was dried in an oven at 80 °C and then used in the next adsorption cycle until the fifth cycle.

3. Results and Discussion

3.1 Material Characterizations

XRD analysis was conducted to assess the crystalline structure of materials. Figure 1(a) shows the crystallization characteristics of SA, CuAl-LDH, and CuAl-LDH/SA samples. As seen from the XRD pattern, the pure state of SA material shows a characteristic peak at an angle of 23.6° and reveals that the structure was weakly crystalline or amorphous. It is a characteristic of carbon-based natural materials [29]. Additional peaks of pure SA are seen in the 25-40° range, mainly associated with compound minerals, especially silica and weddellite [30]. The sharp and symmetric peaks indicate the crystalline nature of the sample. The LDH samples exhibited characteristic peaks at $2\theta = 32.9^{\circ}$, 35.7° , 39.1° , 48.3°, 66.4°, and 68.4° of the hydrotalcite of CuAl-LDH, indicating that CuAl-LDH has been successfully synthesized. The same peak was observed in the CuAl-LDH/SA composite, and the carbon peak appeared at 23.4°, which proved that SA was effectively composited on the LDH structure. The characteristics of the composite material were consistent with those of CuAl-LDH, but the peak decreased. This is due to the composition process with amorphous materials that results in uneven crystallinity of the material, which reduces the crystallinity of the composite [31].

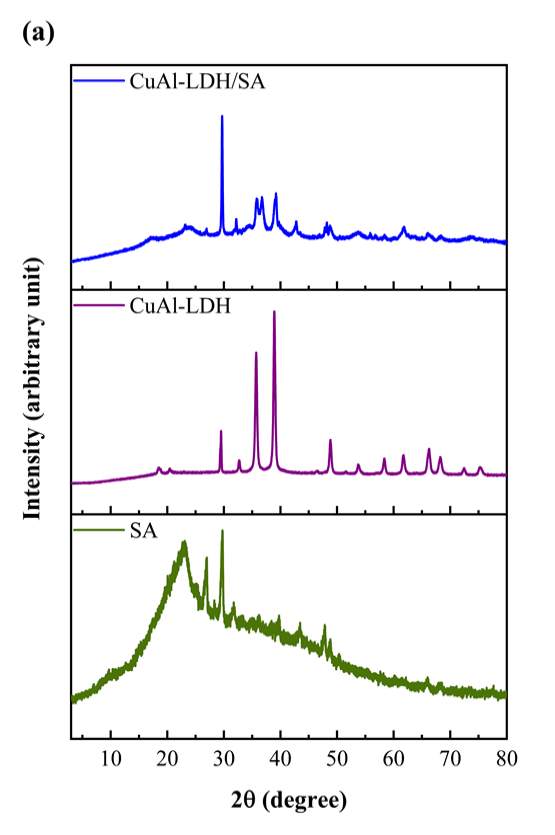
FTIR analysis is predominantly used for functional group materials. The FT-IR spectrum of SA shows a broad absorption peak in the 3400 cm⁻¹ region indicating O-H stretching vibrations

that form intermolecular hydrogen bonds. The absorption peaks observed in the range of 3200-3000 cm⁻¹ suggest the existence of unsaturated C-H stretching vibrations associated with the aromatic ring structure. The absorption peaks associated with the stretching vibrations of the aromatic ring and C=C olefin are observed at 1600 cm⁻¹ and 1450 cm⁻¹, respectively. The pronounced absorption peak observed at 1000 the corresponds to stretching vibrations associated with O-containing functional groups, specifically C-O-C, C-O, and Si-O [24]. The analysis indicates that SA possesses a diverse array of functional groups. The peak observed in CuAl-LDH at 3420 cm⁻¹ shows characteristic stretching and bending vibrations associated with -OH groups and water molecules, both adsorbed and between the layers of adsorbent material. The peaks observed at 1640 and 400-1000 cm-1 for CuAl-LDH are associated with C-C, and M-O stretching vibrations in aromatic hydrocarbons (M = Cu and Al) [31]. The prominent peak observed at 1030-1 cm is attributed to C-O bond stretching vibrations. The absorption band at 1380 cm⁻¹ indicates the nitrate (NO₃) molecules in the LDH material [17]. The FTIR spectrum of CuAl-LDH/SA composite shows the same absorption peak as CuAl-LDH, but at 1040 cm⁻¹ and 1380-1 there is an increase in absorption intensity. This could indicate an increase in the number of functional groups in the composite

material accompanied by the formation of chemical bonds due to the composition of the two materials. This showed that the process of modifying CuAl-LDH material with SA to form composites has been successfully carried out.

BET analysis is used to investigate the specific surface area and pore size distribution of solid materials [32]. The results of the BET analysis are shown in Figure 2(a). In this study, the determination of surface area and pore size of CuAl-LDH/SA composite was carried out by N₂ adsorption-desorption isotherm. According to the results, the BET surface area, pore volume, and pore diameter were found to be 1.07 m²/g, 0.054 cm³/g, and 457.61 nm, respectively. The isotherm curve exhibited characteristics of type IV, displaying a distinct hysteresis loop. The hysteresis curve of these materials resembles that of type H3. The H3 type hysteresis loop, as classified by IUPAC, arises from slit-shaped pores formed by the aggregation of plate-like particles

The thermal decomposition of CuAl-LDH/SA shown in Figure 2(b) can be divided into three main stages. The first stage occurred in a region characterised by relatively low temperatures (below 200 °C) and exhibited minimal mass loss, owing to the evaporation of moisture adsorbed on the outer surface of the materials and the water molecules existing in Cu/Al-LDH interlayer channels or the pores of SA. The weight loss was



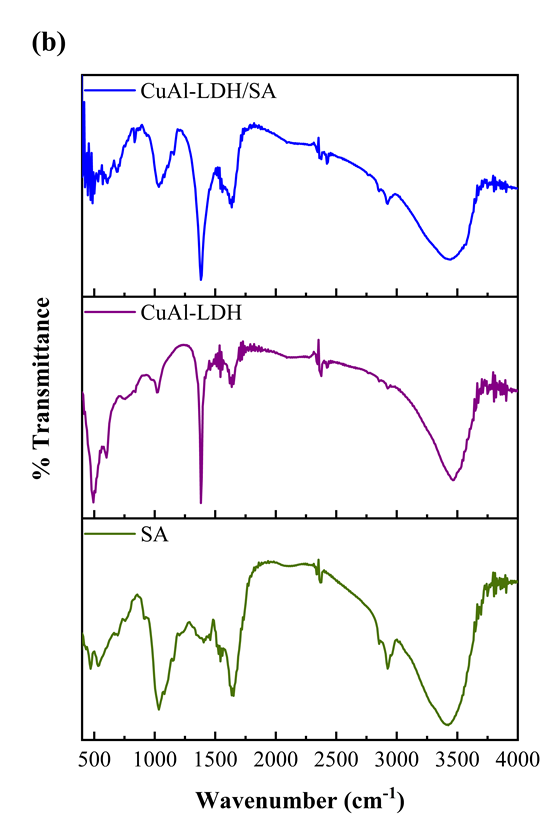


Figure 1. X-ray diffraction patterns (a) and spectrum FT-IR (b) of SA, CuAl-LDH, and CuAl-LDH/SA composite

3.05%. Stage II occurs between 200-500 °C with a weight loss of 10.03%, caused by the dehydroxylation of LDH and the release of volatile substances by the interlayer NO₃- anion. The third stage, from 500 to 1000 °C, was attributed to the decomposition of CuAl-LDH/SA composite with a weight loss of 22.54% [33]. The decomposition profile indicates the ability of the composite to withstand varying temperatures, reflecting its overall stability. The different stages of weight loss demonstrate the structural integrity of the composite. Minimal loss at Stage I indicates effective moisture retention, while weight loss at Stage II confirms the successful incorporation of anions between layers. TG/DTA analysis in this study validated the successful preparation of the composite and confirmed its thermal stability.

Figure 2(c) displays a scanning electron microscopy (SEM) image of the CuAl-LDH/SA composite material, revealing a rough, irregular surface morphology characterized by aggregates of varying sizes and shapes. This surface structure, consistent with findings from other studies [9,34,35], is likely attributed to the interaction between CuAl-LDH and SA on the

composite's surface. The porous, functional grouprich SA particles adhering to the CuAl-LDH matrix introduce additional binding sites, enhancing the material's dye adsorption capacity. This functionalization contributes to a more heterogeneous and accessible surface, which promotes stronger interactions with dye molecules and may significantly improve the overall adsorption efficiency. This unique surface morphology may contribute to an improved adsorption performance by facilitating dye molecule interaction across larger, а heterogeneous surface area.

The pH point of zero charge (pH_{pzc}) for the CuAl-LDH/SA composite was found to be 6.4, as derived from the average of the final pH values measured across an initial pH range of 2 to 11 (refer to Figure 2(d)). Solutions with pH above pH pzc have an unfavorable effect on the adsorption process, as anionic dyes are preferentially adsorbed by positive charges on the material surface [36]. This can be confirmed in the effect of pH on the anionic dye adsorption process in this study. The material's pH_{pzc} at 6.4 indicates that, at pH values below this level, the surface of the adsorbent becomes positively charged, enhancing

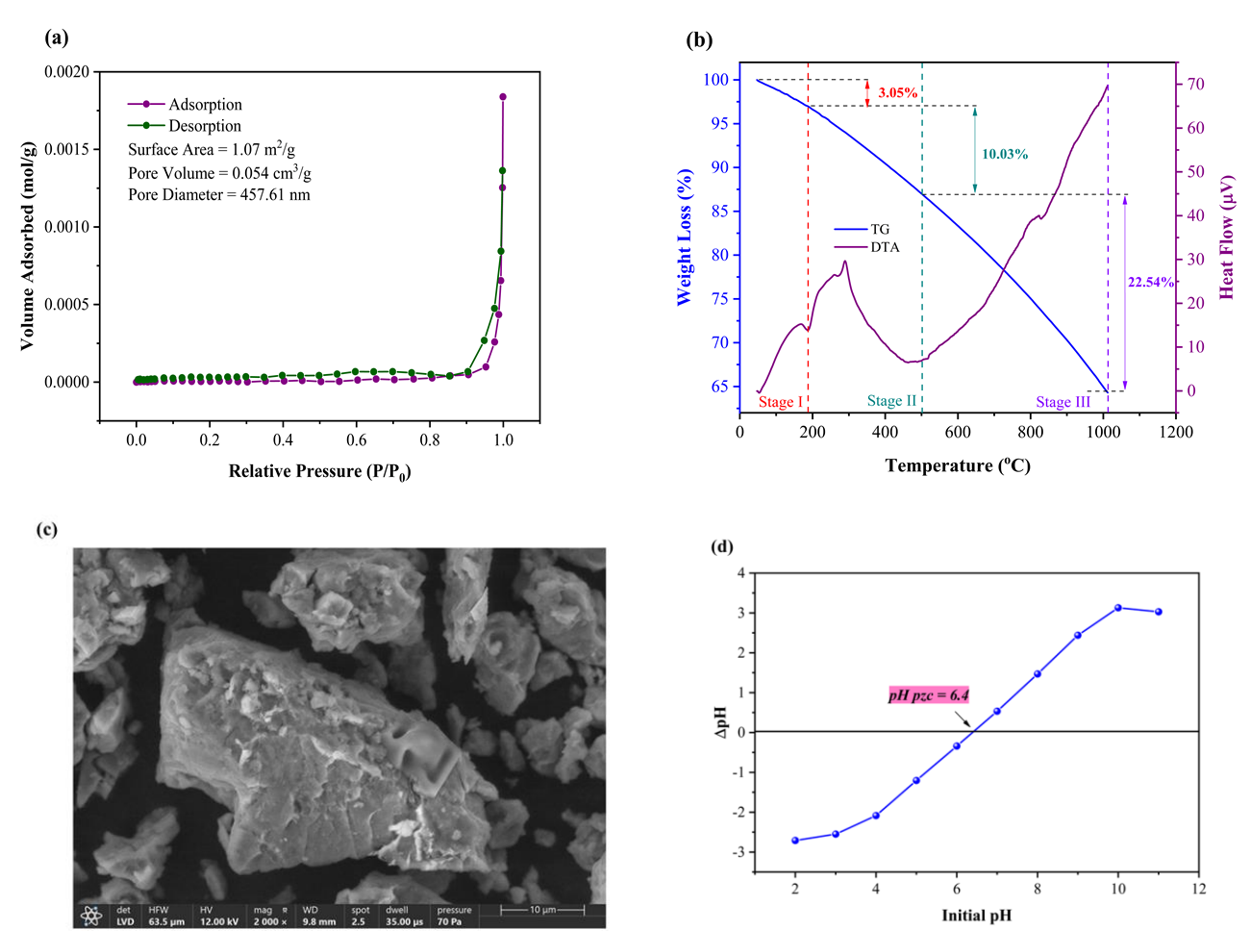


Figure 2. BET analysis (a), TG/DTA curve (b), SEM image (c), and pH_{pzc} (d) of CuAl-LDH/SA composite

electrostatic attraction with anionic dyes. This aligns with the finding that dye adsorption is optimal at acidic pH (pH = 2) in Figure 3(a), where the increased positive surface charge significantly promotes interaction with the negatively charged dye molecules, thus improving adsorption efficiency.

3.2 Effect of pH on Adsorption Process and Adsorption Selectivity

The effect of pH on the adsorption of DY and RR is shown in Figure 3(a). It can be seen that the removal efficiency of both dyes gradually decreased as the pH value increased. Adsorption occurred optimally at pH = 2. The presence of a positive surface charge in the CuAl-LDH/SA composite at lower pH levels facilitated the effective adsorption of negatively charged anionic dyes. The reduction in surface charge as pH values increased resulted in diminished electrostatic attraction heightened and electrostatic repulsion between the CuAl-LDH/SA composite and negatively charged ultimately leading to a decrease in adsorption efficiency. Furthermore, an abundance of OHions in aqueous solutions engaged in competition

with anionic dye molecules. Consequently, the electrostatic interactions were significant in the adsorption process [37].

The effect of pH certainly also influences the selectivity of the adsorption process of the dye mixture DY and RR using the CuAl-LDH/SA composite. Figure 3(b) shows the adsorption process of the dye mixture without pH adjustment, which results in a relatively low removal percentage; however, it can be observed that RR is more selective compared to DY, with percentages of 9.3% and 1.7%, removal respectively. When the pH of the dye mixture DY and RR is adjusted to 2, the removal percentages of both dyes increase to 33.33% (RR) and 32.6% (DY), as shown in Figure 3(c). Although there is an increase in the removal percentages of both, RR achieves a higher removal percentage. Thus, RR is more selective than DY in the adsorption process using the CuAl-LDH/SA composite. RR shows higher adsorption selectivity due to its reactive dye structure, which forms stronger interactions with adsorbents through hydrogen bonding and electrostatic forces, especially via its multiple sulfonic acid groups. Its size and structure also allow better fit within adsorbent

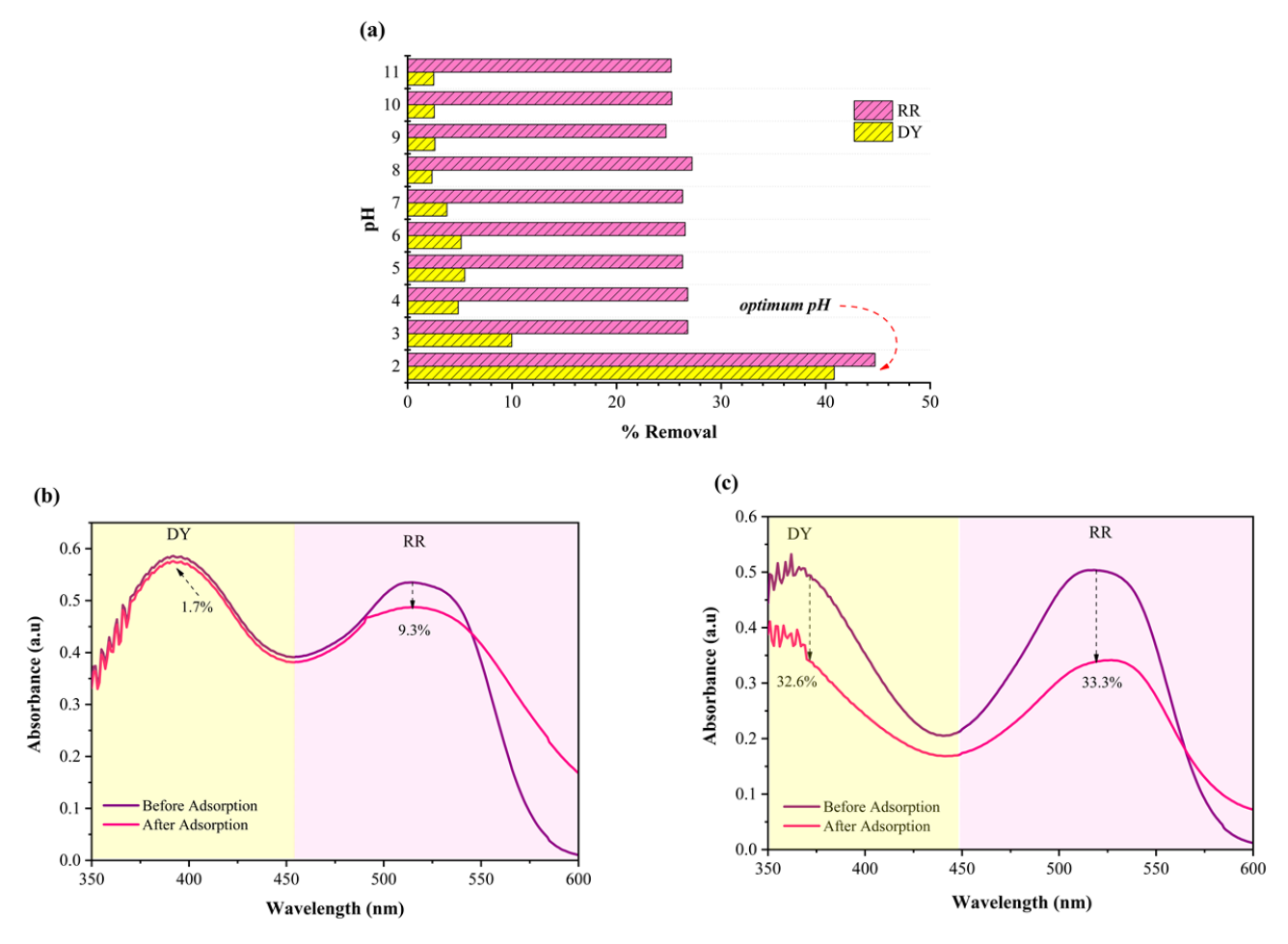


Figure 3. Effect of pH on adsorption of DY and RR (a), scan wavelength on adsorption selectivity of DY and RR mixture, without pH adjustment (b), and pH = 2 (c) using CuAl-LDH/SA composite

pores, enhancing selectivity compared to the simpler structure of DY.

3.3 Adsorption Study

3.3.1 The Adsorption Kinetic

The effect of contact time on the adsorption of RR using CuAl-LDH/SA composite is shown in Figure 4(a). The adsorption capacity increased with increasing contact time and was not significant at more than 120 minutes. The optimum contact time in the adsorption process of RR occurred at 150 min. To analyze the adsorption behavior of RR from aqueous solution using CuAl-LDH/SA composites in this study, pseudo-first-order (PFO), pseudo-second-order (PSO), and intraparticle diffusion were investigated.

Kinetic fittings using the PFO, PSO, and intraparticle diffusion models are presented in Figure 4(b,c,d). The R² value for intraparticle diffusion is higher than the PFO and PSO kinetic models. This indicates that the adsorption process follows the intraparticle diffusion kinetic model. This tendency to follow the intraparticle diffusion kinetics model indicates that the physical characteristics of CuAl-LDH/SA composites, such as pore size and distribution are the main factors affecting the adsorption efficiency and rate. In addition, when the adsorption process follows the

intraparticle diffusion kinetics model, it is more likely to exhibit physisorption [38,39].

3.3.2 Adsorption Isotherm and Thermodynamics

The adsorption isotherm was investigated through a series of adsorption experiments, which conducted with varying initial dye concentrations over a duration of 120 minutes. The adsorption isotherm data were obtained at four distinct temperatures, ranging from 30 to 60 °C. The adsorption data were subjected to analysis through two widely recognised adsorption isotherm models, specifically the Langmuir and Freundlich models. The Langmuir and Freundlich isotherm model data are presented in Table 1. The adsorption process of both dyes showed that the Langmuir isotherm model fits the experimental data better than the Freundlich model, confirmed by the higher correlation coefficient (R2) value of the Langmuir isotherm model. This finding confirmed the monolayer adsorption on the surface [21].

The adsorption capacity of RR using CuAl-LDH/SA composite reached 72.464 mg/g (303 K). Several adsorbents for DY and RR adsorption conducted by researchers are presented in Table 2. The adsorption capacities of the present study are higher than those reported by several authors.

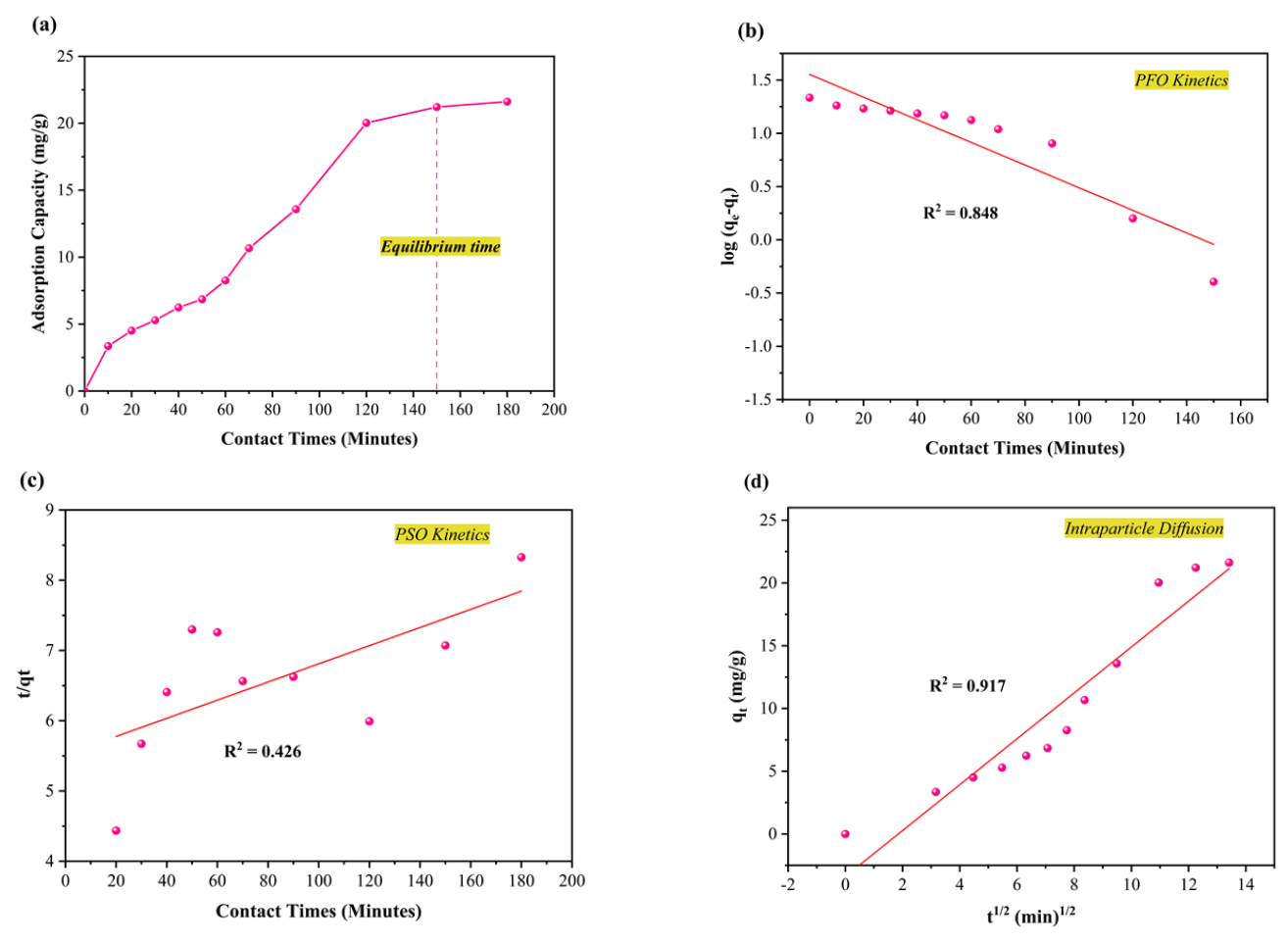


Figure 4. Effect of contact time on the adsorption of RR using CuAl-LDH/SA composite (a), kinetic fitting using the pseudo-first-order model (b), pseudo-second-order model (c), and intraparticle diffusion model (d).

Therefore, it can be concluded that the prepared CuAl/BC shows great potential as an adsorbent for DY and RR dyes.

The thermodynamic parameter data are tabulated in Table 3. The adsorption of RR exhibited positive values for both ΔH and ΔS calculations, suggesting that the adsorption process is characterized by an endothermic nature and an enhanced degree of randomness in the adsorption operation. RR adsorption results showed negative values of Gibbs free energy (ΔG) at all temperatures, indicating that the adsorption process was spontaneous. adsorption results for RR indicate that the Gibbs free energy (ΔG) becomes progressively more negative with increasing temperature, signifying that the adsorption process is increasingly spontaneous at higher temperatures. This indicates that the adsorption process occurs naturally at higher temperatures. The enthalpy values for RR adsorption are <40 kJ/mol and ΔG values are in the range of 0 to -20 kJ/mol indicating the adsorption process occurs by [9]. physisorption Thus, $_{
m the}$ adsorption mechanism that occurs between CuAl-LDH/SA and the dye includes surface interaction and pore filling.

3.4 Adsorbent Regeneration Study

Regeneration provides significant benefits, including the prolongation of the adsorbent's operational lifespan, decreased operational expenses linked to the new adsorbents, diminished necessity for ongoing production of

Table 1. Adsorption isotherm for RR adsorption using CuAl-LDH/SA composite

T (K)	$Q_{ m max}$	Langmuir	Freundlich
	(mg/g)	\mathbb{R}^2	\mathbb{R}^2
303	72.464	0.883	0.854
313	65.359	0.938	0.872
323	64.103	0.972	0.906
333	65.789	0.982	0.927

adsorbents, and mitigated effects related to the manufacturing and disposal of increased quantities of adsorbent materials. Furthermore, adsorption that is based on regeneration underscores the importance of resource utilization and the minimization of waste. Considering these advantages, it is crucial to develop and implement effective regeneration methods [46,47]. The desorption method employed in this study, using distilled water with ultrasonic assistance, prioritizes environmental sustainability over maximum desorption efficiency. While it is known that organic or inorganic reagents could enhance desorption by breaking down dye-adsorbent interactions more effectively, we have selected distilled water to avoid potential chemical waste and environmental harm. Ultrasonic equipment aids this process by disrupting physical interactions and facilitating dye release without introducing additional chemicals.

This study was conducted successfully utilizing the ultrasonic method. The regeneration ability of the CuAl-LDH/SA in the adsorption process of RR is shown in Figure 5. As the regeneration cycle increases, there is a decrease in the percent removal that is not so significant. Based on these results, it can be concluded that the CuAl-LDH/SA composite material can be regenerated for 4 cycles with a percent removal of RR of 29.32%. In the fifth cycle, the percent removal has decreased below 50% from the first cycle of regeneration.

Table 3. Thermodynamic parameters of RR adsorption (C_0 : 60 mg/L) using CuAl-LDH/SA composite.

T (K)	ΔH (kJ/mol)	ΔS (J/mol.K)	ΔG (kJ/mol)
303	9.144	0.029	0.206
313			-0.089
323			-0.384
333			-0.679

Table 2. Previous studies in the literature report on RR adsorption

Materials	Adsorption Capacity (mg/g)	References
CuAl-LDH/SA	72.464	This work
Black binary Ni-Co oxide nano-powder	45.25	[40]
$Anabaena\ sphaerica ext{-} \mathrm{Fe}_3\mathrm{O}_4$	63.9	[41]
Nanocrystalline FeNi alloy powder	80.97	[42]
O-carboxymethyl chitosan-N-lauryl/γ-Fe ₂ O ₃	216	[43]
magnetic nanoparticles		
Rice husk ash	11.83	[44]
Pumice powder	38.9	[45]

3.5 Adsorption Mechanism of RR with CuAl-SA composite

The mechanism of RR adsorption using CuAl-SA composite was investigated through multiple experiments in this study, encompassing pH, isotherm, thermodynamics, kinetics, and complemented by material characterization conducted prior to and following the adsorption process. The kinetics, isotherms, thermodynamics data indicate that the adsorption process takes place by physisorption and chemisorption, so there are physical and chemical interactions occurring between the material and the dye. The pH findings further indicate that the optimal performance for RR removal using CuAl/SA composites is achieved at pH levels below pHzpc, which can be discussed in this way. At pH levels below pH_{pzc}, the -COOH, C-O-H, and C-O functional groups present on the materials

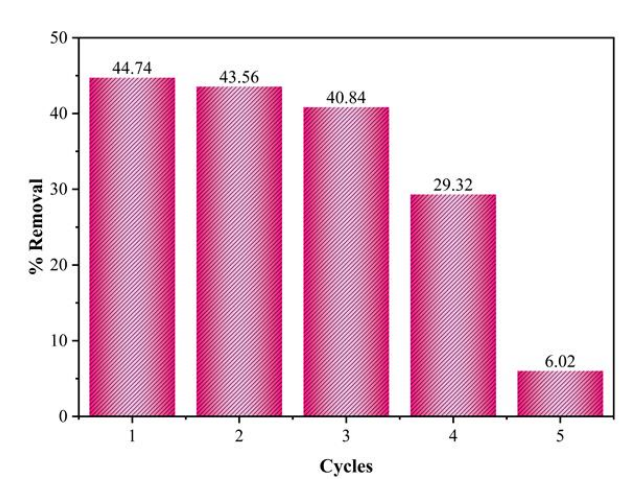


Figure 5. Effects of adsorbent regeneration on RR removal using CuAl-LDH/SA composite

acquire a positive charge due to electrostatic interactions with the positively charged RR molecules [48]. RR anionic dye has N and O atoms, which can form hydrogen bonds with H atoms in the structure of CuAl/SA composite. In addition, the C=C bond in the CuAl/SA composite can form π - π interactions with the benzene ring in the RR dye structure [49]. Based on these studies, an illustration of the adsorption mechanism between CuAl/SA composites and RR dyes is shown in Figure 6.

To confirm the adsorption mechanism, this study conducted FT-IR characterization of CuAl/SA composites before and after RR adsorption (Figure 7). The peak shifts and changes in intensity indicate that there are functional group interactions between RR and Identified CuAl/SA composite materials. functional groups such as O-H (3422 cm⁻¹), C=C (1630 cm⁻¹), C=O (1052 cm⁻¹), and M=O (486 cm⁻¹) participate in the adsorption process. The shift of the O-H peak can be attributed to the hydrogen bonding interactions that occur. The intensity change and peak shift at 1380 cm⁻¹ identified that the interaction between the sulfonate group (-SO₃-) on the dye and the nitrate group (NO₃-) on the CuAl/SA composite played an important role in the spectrum change, where the sulfonate anion replaced the nitrate anion in the interlayer so that ion exchange occurred. The wave number shift and intensity change around 1660 cm⁻¹ indicate the interaction between C=C bonds (in aromatic structures or double bonds from dyes) and the surface of CuAl/SA composites, which can occur through π - π stacking interactions or changes in C=C vibrations due to interaction with the material surface. So from this study it can be

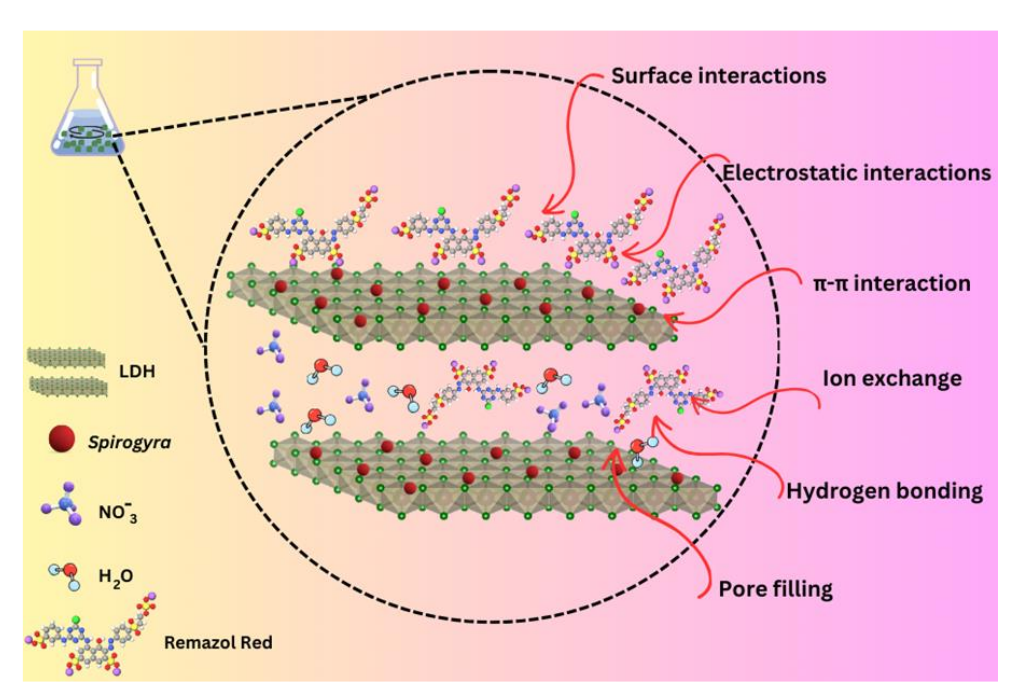


Figure 6. The illustration of mechanism adsorption on RR and CuAl-LDH/SA composite.

concluded that there are physical and chemical interactions that occur in the RR adsorption process including surface interactions, pore filling, electrostatic interactions, π - π interactions, ion exchange, and hydrogen bonding.

This research mainly focused on the adsorption efficiency and selectivity of CuAl/SA composites for anionic dyes, specifically RR and DY, under controlled laboratory conditions. However, limitations include the lack of toxicity assessment for both the composite and the adsorbed dyes, as well as the absence of long-term stability tests under various environmental conditions. Future research should address these limitations by investigating $_{
m the}$ adsorption performance of the composites in complex wastewater matrices. In addition, exploring the regeneration capacity of the composite over multiple cycles will enhance its practical applicability in wastewater treatment.

4. Conclusions

The successfully prepared CuAl-LDH/SA composite material via coprecipitation and hydrothermal method produced maximum capacity with optimum conditions on RR adsorption of 72.464 mg/g (pH = 2, 150 min, 303K). RR exhibits higher selectivity than DY in

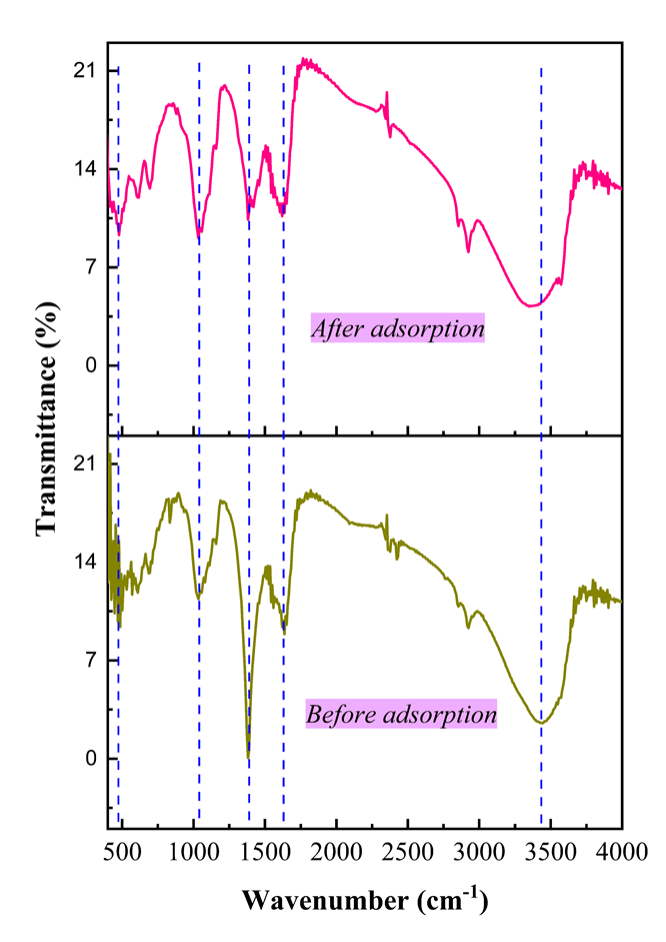


Figure 9. FT-IR Spectra of CuAl-LDH/SA composite before and after adsorption of RR

the adsorption process. The adsorption process followed the intraparticle diffusion kinetics model and Langmuir isotherm. Thermodynamic studies showed that the adsorption was endothermic and spontaneous. CuAl-LDH/SA composite material can be regenerated for 4 cycles with a percent removal of 29.32%. Adsorption that occurs includes physisorption and chemisorption. Based on this study, the CuAl/SA composite material demonstrates significant potential for the removal of anionic dyes from aqueous media.

Acknowledgment

The authors extend their thanks to the Research Centre of Inorganic Materials and Coordination Complexes at Universitas Sriwijaya for their significant contributions through discussions, support, and instrumental analysis throughout this research.

CRediT Author Statement

Alfan Wijaya: Conceptualization, Investigation, Writing – Original draft, Software. Laila Hanum: Methodology, Visualization, Validation, Data Acuration. Elda Melwita: Methodology, Validation, Visualization, Conceptualization. Aldes Lesbani: Methodology, Conceptualization, Writing – review & editing, Supervision. All authors have read and agreed to the published version of the manuscript.

References

- [1] Jung, S., Jung, M., Yoon, J., Kim, J., Jin, H., Won, H. (2024). Chitosan-derived activated carbon / chitosan composite beads for adsorptive removal of methylene blue and acid orange 7 dyes. Reactive and Functional Polymers, 204 (August), 106028. DOI: 10.1016/j.reactfunctpolym.2024.106028.
- [2] Tian, W., Zhou, H., Liu, Y., Yang, Z., Li, Q., Qi, F., Yu, Y. (2024). A robust polypyrrole nanofibrous membrane for versatile applications: Oil-water separation and dye removal. *Journal of Environmental Chemical Engineering*, 12 (3), 113109. DOI: 10.1016/j.jece.2024.113109.
- [3] Wang, H., Chen, C., Dai, K., Xiang, H., Kou, J., Guo, H., Ying, H., Chen, X., Wu, J. (2024). Selective adsorption of anionic dyes by a macropore magnetic lignin-chitosan adsorbent. International Journal of Biological Macromolecules, 269 (P2), 131955. DOI: 10.1016/j.ijbiomac.2024.131955.
- [4] Krupková, O., Dušek, L., Cuhorka, J., Soares, G., Kuchtová, G., Mikulášek, P., Bendová, H. (2024). Removal of textile dye reactive blue 49 from wastewater and dye baths by membrane separation and subsequent photo-Fenton reaction, UV-C and UV-C/H2O2. Journal of Water Process Engineering, 65 (June). DOI: 10.1016/j.jwpe.2024.105735.

- [5] Duan, Y., Zhao, J., Qiu, X., Deng, X., Ren, X., Ge, W., Yuan, H. (2022). Coagulation performance and floc properties for synchronous removal of reactive dye and polyethylene terephthalate microplastics. *Process Safety and Environmental Protection*, 165(June), 66–76. DOI: 10.1016/j.psep.2022.07.010.
- [6] Muniasamy, S.K., Alobaid, A.A., Warad, I., Ravindiran, G. (2023). Removal of Brilliant Green dye in aqueous solution using synthetic coagulation and flocculation technique. *Desalination and Water Treatment*, 314, 231– 240. DOI: 10.5004/dwt.2023.30093.
- [7] Feng, X., Li, X., Su, B. (2023). Photocatalytic degradation performance of antibiotics by peanut shell biochar anchored NiCr-LDH nanocomposites fabricated by one-pot hydrothermal protocol. Colloids and Surfaces A: Physicochemical and Engineering Aspects, 666(March), 131337. DOI: 10.1016/j.colsurfa.2023.131337.
- [8] Li, X. fang, Li, R. xian, Wang, K. xin, Feng, X. qiang (2023). Highly synergic adsorption and photocatalytic degradation of walnut shell biochar/NiCr-layered double hydroxides composite for Methyl orange. Journal of Industrial and Engineering Chemistry, 126, 270–282. DOI: 10.1016/j.jiec.2023.06.017.
- [9] Wijaya, A., Zahara, Artha, Zaqiya, Siregar, P.M.S.B.N., Ahmad, N., Amri, A., Palapa, N.R., Mohadi, R., Lesbani, A. (2024). Cellulose-supported Ni/Al Layered Double Hydroxide (LDH) as Unique Adsorbents for Malachite Green Dye Removal in Aqueous Solutions. Iranian Journal of Chemistry and Chemical Engineering, 43(4), 1566–1578. DOI: 10.30492/ijcce.2024.1983141.5779.
- [10] Amri, A., Wibiyan, S., Wijaya, A., Ahmad, N., Mohadi, R., Lesbani, A. (2024). Efficient Adsorption of Methylene Blue Dye Using Ni/Al Layered Double Hydroxide-Graphene Oxide Composite. Bulletin of Chemical Reaction Engineering & Catalysis, 19(2), 181–189. DOI: 10.9767/bcrec.20121.
- [11] Li, Y., Liu, H., Nie, R., Li, Y., Li, Q., Lei, Y., Guo, M., Zhang, Y. (2024). Highly efficient adsorption of anionic dyes on a porous graphene oxide nanosheets/chitosan composite aerogel. Industrial Crops and Products, 220(January), 119146. DOI: 10.1016/j.indcrop.2024.119146.
- [12] Mujtaba, G., Hai, A., Ul Hassan Shah, M., Ullah, A., Anwar, Y., Shah, F., Daud, M., Hussain, A., Ahmed, F., Banat, F. (2024). Potential of Capparis decidua plant and eggshell composite adsorbent for effective removal of anionic dyes from aqueous medium. *Environmental Research*, 247(December 2023), 118279. DOI: 10.1016/j.envres.2024.118279.
- [13] Badaruddin, M., Ahmad, N., Fitri, E.S., Lesbani, A., Mohadi, R. (2022). Hydrochar and Humic Acid as Template of ZnAl Layered Double Hydroxide for Adsorption of Phenol. Science and Technology Indonesia, 7(4), 492–499. DOI: 10.26554/sti.2022.7.4.492-499.

- [14] Palapa, N.R., Amri, A., Hanifah, Y. (2023). Potential Indonesian Rice Husk for Wastewater Treatment Agricultural Waste Preparation and Dye Removal Application. Indonesian Journal of Environmental Management and Sustainability, 7(4), 160–165. DOI: 10.26554/ijems.2023.7.4.160-165.
- [15] Taher, T., Munandar, A., Mawaddah, N., Wisnubroto, M.S., Mega, P., Bahar, S., Siregar, N., Rahayu, N., Lesbani, A., Gusti, Y. (2023). Synthesis and characterization of montmorillonite Mixed metal oxide composite and its adsorption performance for anionic and cationic dyes removal. *Inorganic Chemistry Communications*, 147(October 2022), 110231.
- [16] Ahmad, N., Marlan, A.R., Negara, S.P.J. (2024). Insight of Anionic Dyes Adsorption from Their Aqueous Solutions onto MgAl LDH/Lignin: Characterization and Isotherm Studies. Indonesian Journal of Material Research, 2(2), 40–46.
- [17] Normah, N., Lesbani, A. (2024). Comparison of LDH-Organic/Inorganic Compound Modified Materials as Adsorbents for Heavy Metal Adsorption: Characteristic Structure and Adsorption Mechanism. Bulletin of Chemical Reaction Engineering & Catalysis, 19(2), 327–339. DOI: 10.9767/bcrec.20160.
- [18] Dolfini, N., Viotti Moreira, P.V., Moreira, W.M., Scheufele, F.B., Arroyo, P.A., Pereira, N.C. (2024). LDH/Alginate composite for anionic dye adsorption: synthesis, mechanisms and modeling. Separation and Purification Technology, 351(May) DOI: 10.1016/j.seppur.2024.128073.
- [19] Ahmad, N., Wijaya, A., Arsyad, F.S., Royani, I., Lesbani, A. (2024). Layered double hydroxidefunctionalized humic acid and magnetite by hydrothermal synthesis for optimized adsorption of malachite green. *Kuwait Journal of Science*, 51(2), 100206. DOI: 10.1016/j.kjs.2024.100206.
- [20] Cruz, E.D., Missau, J., Collinson, S.R., Tanabe, E.H., Bertuol, D.A. (2023). Efficient removal of congo red dye using activated lychee peel biochar supported Ca-Cr layered double hydroxide. *Environmental Nanotechnology, Monitoring and Management*, 20(May), 100835. DOI: 10.1016/j.enmm.2023.100835.
- [21] Palapa, N.R., Taher, T., Rahayu, B.R., Mohadi, R., Rachmat, A., Lesbani, A. (2020). CuAl LDH/Rice husk biochar composite for enhanced adsorptive removal of cationic dye from aqueous solution. Bulletin of Chemical Reaction Engineering & Catalysis, 15 (2), 525–537. DOI: 10.9767/bcrec.15.2.7828.525-537.
- Han, W., Hao, H., Zhang, Q., Shao, Z. (2023). [22] Journal of Environmental Chemical Engineering Activated biochar loaded CuAl-layered double hydroxide composite for the removal of aniline aerofloat in wastewater: Synthesis characterization, and adsorption mechanism. *Journal* of EnvironmentalChemicalEngineering, 11 (2),109293. DOI: 10.1016/j.jece.2023.109293.

- [23] Normah, N., Juleanti, N., Mega, P., Bahar, S., Siregar, N., Wijaya, A. (2021). Size Selectivity of Anionic and Cationic Dyes Using LDH Modified Adsorbent with Low-Cost Rambutan Peel to Hydrochar. Bulletin of Chemical Reaction Engineering & Catalysis, 16 (4), 869–880. DOI: 10.9767/bcrec.16.4.12093.869-880.
- [24] Li, X., Liu, W., Zhang, J., Wang, Z., Guo, Z., Ali, J., Wang, L., Yu, Z., Zhang, X., Sun, Y. (2024). Effective removal of microplastics by filamentous algae and its magnetic biochar: Performance and mechanism. *Chemosphere*, 358 (February), 142152. DOI: 10.1016/j.chemosphere.2024.142152.
- [25] Jiat, X., Chyuan, H., Ooi, J., Ling, K., Chai, T., Chen, W., Sik, Y. (2022). Engineered macroalgal and microalgal adsorbents: Synthesis routes and adsorptive performance on hazardous water contaminants. *Journal of Hazardous Materials*, 423 (PA), 126921. DOI: 10.1016/j.jhazmat.2021.126921.
- [26] Liu, Y., Zhao, J., Chen, S., Yao, J., Liu, J. (2024). Removal of arsenic from realgar-containing water by Spirogyra: Implications for in situ remediation of arsenic in the mine area. *Applied Geochemistry*, 160 (December 2023), 105873. DOI: 10.1016/j.apgeochem.2023.105873.
- [27] Yahya, M.D., Muhammed, I.B., Obayomi, K.S., Olugbenga, A.G., Abdullahi, U.B. (2020). Optimization of fixed bed column process for removal of Fe(II) and Pb(II) ions from thermal power plant effluent using NaoH-rice husk ash and Spirogyra. *Scientific African*, 10, e00649. DOI: 10.1016/j.sciaf.2020.e00649.
- [28] Riaz, S., Rehman, A. ur, Akhter, Z., Najam, T., Hossain, I., Karim, M.R., Assiri, M.A., Shah, S.S.A., Nazir, M.A. (2024). Recent advancement in synthesis and applications of layered double hydroxides (LDHs) composites. *Materials Today Sustainability*, 27 (May), 100897. DOI: 10.1016/j.mtsust.2024.100897.
- [29] Bekirogullari, M., Abut, S., Duman, F., Hansu, T.A. (2024). Dual-function macroalgae biochar: Catalyst for hydrogen production and electrocatalyst. Fuel, 362 (December 2023), 130920. DOI: 10.1016/j.fuel.2024.130920.
- [30] Salim, M.H., Kassab, Z., Ablouh, E. houssaine, Sehaqui, H., Aboulkas, A., Bouhfid, R., Qaiss, A.E.K., El Achaby, M. (2022). Manufacturing of macroporous cellulose monolith from green macroalgae and its application for wastewater treatment. *International Journal of Biological Macromolecules*, 200 (September 2021), 182–192. DOI: 10.1016/j.ijbiomac.2021.12.153.
- [31] Han, W., Hao, H., Zhang, Q., Shao, Z. (2023). Activated biochar loaded CuAl-layered double hydroxide composite for the removal of aniline aerofloat in wastewater: Synthesis, characterization, and adsorption mechanism. EnvironmentalChemicalJournalof Engineering, 11 (2),109293. DOI: 10.1016/j.jece.2023.109293.

- [32] Khodakarami, M., Dehghan, G., Rashtbari, S., Amini, M. (2024). Catalytic removal of malachite green from aqueous solution by a peroxidase-mimicking Cu-Al layered double hydroxide nanoparticle: Synthesis, characterization, and application. Applied Catalysis A: General, 670(January), 119563. DOI: 10.1016/j.apcata.2024.119563.
- [33] Zhang, J., Lu, W., Zhan, S., Qiu, J., Wang, X., Wu, Z., Li, H., Qiu, Z., Peng, H. (2021). Adsorption and mechanistic study for humic acid removal by magnetic biochar derived from forestry wastes functionalized with Mg/Al-LDH. Separation and Purification Technology, 276 (June), 119296. DOI: 10.1016/j.seppur.2021.119296.
- [34] de Jesus, A.S., Ferreira, G.M.D., Ferreira, G.M.D., Souza, T.F., Siqueira, K.P.F., Nogueira, A.E., Barbosa Mageste, A. (2024). Composite of Organo-LDH and biochar for diclofenac sodium removal from aqueous solutions. *Materials Chemistry and Physics*, 328 (August) DOI: 10.1016/j.matchemphys.2024.129919.
- [35] Zhu, R., Yuan, W., Cheng, J., Qiu, X. (2024). FeAl-LDH-modified biochar (FeAl-LDH@BC): A high-efficiency passivator for hexavalent chromium (Cr(VI)) reduction and immobilization in contaminated soil. Sustainable Chemistry for the Environment, 8(July), 100169. DOI: 10.1016/j.scenv.2024.100169.
- [36] Araújo, Y.M. De, Medeiros, R., Heriberto, J., Tinôco, J.D. (2024). Functionalized graphene oxide as an adsorbent material for endocrine disruptor 4-octylphenol. *Desalination and Water Treatment*, 318 (April), 100346. DOI: 10.1016/j.dwt.2024.100346.
- [37] Song, G., Fan, W., Zhang, J., Xue, T., Shi, Y., Sun, Y., Ding, G. (2024). Applied Surface Science Adsorption of anionic dyes from aqueous solutions by a novel CTAB / MXene / carbon nanotube composite: Characterization , experiments , and theoretical analysis. Applied Surface Science, 661 (April), 160036. DOI: 10.1016/j.apsusc.2024.160036.
- [38] Abdelmegeed, A.F., Sayed, M., Abbas, M., Abdel Moniem, S.M., Farag, R.S., Sayed, A.Z., Naga, S.M. (2024). Hydroxyapatite-magnetite nanocomposites: Synthesis and superior adsorption properties for lead ion removal, with insights into intraparticle diffusion, kinetic modeling, and phase dependency. Ceramics International, 50 (19), 36074–36087. DOI: 10.1016/j.ceramint.2024.06.420.
- [39] Farhat, Z., Kumar, A., Das, C. (2024). Fabrication of used-tea embedded alginate beads for cationic dye remediation: Synergistic effect of surface adsorption and intraparticle diffusion. Surfaces and Interfaces, 51 (June), 104601. DOI: 10.1016/j.surfin.2024.104601.

- [40] El Boraei, N.F., Ibrahim, M.A.M. (2019). Black binary nickel cobalt oxide nano-powder prepared by cathodic electrodeposition; characterization and its efficient application on removing the Remazol Red textile dye from aqueous solution. *Materials Chemistry and Physics*, 238 (November 2018), 121894. DOI: 10.1016/j.matchemphys.2019.121894.
- [41] Abdel-Wahed, M.S., El-Kalliny, A.S., Shehata, F.A., Abd El-Aty, A.M., Gad-Allah, T.A. (2023). One-pot green synthesis of magnetic adsorbent via Anabaena sphaerica and its performance towards Remazol Red dye removal from aqueous media. *Chemical Engineering Science*, 279 (February), 118939. DOI: 10.1016/j.ces.2023.118939.
- [42] El, N.F., Ibrahim, M.A.M., Naghmash, M.A. (2022). Journal of Physics and Chemistry of Solids Nanocrystalline FeNi alloy powder prepared by electrolytic synthesis: characterization and its high efficiency in removing Remazol Red dye from aqueous solution. Journal of Physics and Chemistry of 167(February), 110714. DOI: 10.1016/j.jpcs.2022.110714.
- [43] Albertina, C., Debrassi, A., Nedelko, N., Anna, S. (2019). Adsorption of the dye Remazol Red 198 (RR198) by O-carboxymethylchitosan-N-lauryl / c-Fe2O3 magnetic nanoparticles. 3444–3453. DOI: 10.1016/j.arabjc.2015.08.028.
- [44] Costa, J.A.S., Paranhos, C.M. (2019). Evaluation of rice husk ash in adsorption of Remazol Red dye from aqueous media. SN Applied Sciences, 1(5), 1–8. DOI: 10.1007/s42452-019-0436-1.
- [45] Gürses, A., Güneş, K., Şahin, E., Açıkyıldız, M. (2023). Investigation of the removal kinetics, thermodynamics and adsorption mechanism of anionic textile dye, Remazol Red RB, with powder pumice, a sustainable adsorbent from waste water. Frontiers in Chemistry, 11(June), 1–14. DOI: 10.3389/fchem.2023.1156577.

- [46] Sithole, T. (2024). South African Journal of Chemical Engineering A review on regeneration of adsorbent and recovery of metals: Adsorbent disposal and regeneration mechanism. South African Journal of Chemical Engineering, 50 (July), 39–50. DOI: 10.1016/j.sajce.2024.07.006.
- [47] Vakili, M., Cagnetta, G., Deng, S., Wang, W., Gholami, Z., Gholami, F., Dastyar, W., Mojiri, A., Blaney, L. (2024). Regeneration of exhausted adsorbents after PFAS adsorption: A critical review. Journal of Hazardous Materials, 471 (April), 134429. DOI: 10.1016/j.jhazmat.2024.134429.
- [48] Suhaimi, A., Abdulhameed, A.S., Jawad, A.H., Yousef, T.A., Al Duaij, O.K., ALOthman, Z.A., Wilson, L.D. (2022). Production of large surface area activated carbon from a mixture of carrot juice pulp and pomegranate peel using microwave radiation-assisted ZnCl2 activation: An optimized removal process and tailored adsorption mechanism of crystal violet dye. Diamond and Related Materials, 130 (October), 109456. DOI: 10.1016/j.diamond.2022.109456.
- [49] Peighambardoust, S.J., Imani Zardkhaneh, S., Foroughi, M., Foroutan, R., Azimi, H., Ramavandi, B. (2024). Effectiveness of polyacrylamide-g-gelatin/ACL/Mg-Fe LDH composite hydrogel as an eliminator of crystal violet dye. *Environmental Research*, 258 (May), 119428. DOI: 10.1016/j.envres.2024.119428.